THE ASTROPHYSICAL JOURNAL, 520:L5–L8, 1999 July 20

MASSIVE COOLING FLOW CLUSTERS INHABIT CROWDED ENVIRONMENTS

CHRIS LOKEN
Department of Physics and Astronomy, University of Missouri, Columbia, MO 65211; cloken@hades.physics.missouri.edu
ADRIAN L. MELOTT
Department of Physics and Astronomy, University of Kansas, Lawrence, KS 66045; melott@kusmos.phsx.ukans.edu
AND
CHRISTOPHER J. MILLER
Department of Physics and Astronomy, University of Maine, Orono, ME 04469; chrism@perseus.umephy.maine.edu
Received 1999 April 7; accepted 1999 May 17; published 1999 June 10

ABSTRACT

With the availability of large-scale redshift survey data, it is now becoming possible to explore correlations between large-scale structure and the properties and morphologies of galaxy clusters. We investigate the spatial distributions of a 98% complete, volume-limited sample of nearby ($z < 0.1$) Abell clusters with well-determined redshifts and find that cooling flow clusters with high mass accretion rates have nearest neighbors which are much closer than those of other clusters in the sample (at the 99.8% confidence level) and reside in more crowded environments out to 60 h_{50}^{-1} Mpc. Several possible explanations of this effect are discussed.

Subject headings: cooling flows — galaxies: clusters: general — large-scale structure of universe

1. INTRODUCTION

Intriguing correlations between cluster properties and larger scale structures have been noted over the past two decades. For example, the major axes of Abell clusters may be aligned with nearby clusters (see, e.g., Bingelli 1982; Plionis 1994), X-ray substructure within clusters appears to point to neighboring Abell clusters (West, Jones, & Forman 1995), and the tails of wide-angle tailed (WAT) radio sources within clusters tend to be aligned with the long axis of the nearest supercluster (Novikov et al. 1999). All these alignment effects are broadly consistent with the scenario of hierarchical structure formation whereby clusters form through the flow of material along sheets and filaments (see, e.g., Shandarin & Klypin 1984; Pauls & Melott 1995; Bond, Kofman, & Pogosyan 1996; Colberg et al. 1999). Here we investigate another possible link between cluster properties and larger scale structures: the environments within which cooling flow clusters are located.

Cluster cooling flows are believed to result when gas within the central ~100 kpc cools radiatively on a timescale less than a Hubble time; the resultant decrease in pressure allows gas to flow toward the core (see, e.g., the review of Fabian 1994). Several groups have estimated that 60%–90% of clusters contain cooling flows (Edge, Stewart, & Fabian 1992; White, Jones, & Forman 1997; Peres et al. 1998) with mass deposition rates (obtained by detailed deprojection analysis of their X-ray images) ranging from a few to more than 1000 $M_\odot$ yr^{-1}. The environmental factors which determine whether or not a given cluster will develop a cooling flow are still unclear and have not been properly addressed by numerical simulations. However, the development of a strong cooling flow was observed in the single cluster simulation of Katz & White (1993), and detailed one-dimensional simulations incorporating many realistic effects suggest that strong cooling flows are a natural outcome of cluster formation over a wide range in masses (Knight & Ponman 1997).

Although cooling flows may be a generic feature of cluster formation, it appears that the recent merger history of a cluster is closely linked to the existence and/or strength of a cooling flow. McGlynn & Fabian (1984) and Fabian & Daines (1991) suggested that cooling flows may be disrupted by cluster mergers. This is supported by the fact that there are no cooling flows in several massive clusters which appear to have undergone recent mergers (e.g., Coma: Burns et al. 1994; A2255: Burns et al. 1995). Unfortunately, the observational picture is not entirely clear as there are also cooling flow clusters which appear to have undergone a merger (e.g., A1664: Allen et al. 1996; A2597: Sarazin et al. 1995). Nonetheless, the observations are consistent with a scenario in which recent and/or massive mergers tend to disrupt any preexisting cooling flow. For example, Buote & Tsai (1996) demonstrated that cooling flow strength is anticorrelated with the degree of X-ray substructure (which is likely a measure of recent merger activity). Recent numerical simulations (Burns et al. 1997; Gomez et al. 1999) of cooling flow mergers indicate that high-M flows are more difficult to disrupt than low-M flows and that the likelihood of disrupting a given cooling flow increases with the mass of the infalling cluster.

To date, there has been no systematic investigation of the large-scale environments within which cooling flow clusters are found. A possible connection between large-scale structure and cluster cooling flows comes from the evidence that mergers can disrupt cooling flows which, in turn, suggests that massive cooling flows have been relatively undisturbed for some time. As Abell clusters are thought to delineate the supercluster distribution rather well (see, e.g., Bahcall, Cen, & Gramann 1994), we decided to investigate the spatial distribution of Abell clusters around cooling flows.

2. PROCEDURE

2.1. *The Abell Cluster Sample*

We began by constructing a complete sample of all rich Abell/ACO clusters (Abell 1958; Abell, Corwin, & Olowin 1989) with $R \geq 1$, $m_{10} \leq 17.0$, $|b| \geq 30°$, and spectroscopically determined redshifts $0.012 \leq z \leq 0.10$ (where R is Abell's richness class and m_{10} is the magnitude of the 10th brightest galaxy within the cluster). The cut in Galactic latitude rejects regions of the sky where obscuration and poor sampling may plague the ACO catalog, while our magnitude limit corresponds to $z \sim 0.13$ assuming an m_{10}-z relationship (see, e.g., Batuski &

Burns 1985). The total number of ACO clusters satisfying these cuts is 284, of which we kept the 277 with measured redshifts. The majority of the cluster redshifts come from the ESO Nearby Abell Cluster Survey (Katgert et al. 1996) and the MX Northern Abell Cluster Survey (Slinglend et al. 1998), although ~50 are unpublished redshifts from Miller et al. (1999b).

It is important to note the level of completeness (98%) and quality of this Abell/ACO data set. Miller et al. (1999a) and Peacock & West (1992) have shown that $R \geq 1$ Abell/ACO clusters suffer much less from spurious cluster selection (due to line-of-sight anisotropies) than do samples containing $R = 0$ clusters. By limiting the samples to $R \geq 1$ clusters, we are sacrificing some poorer clusters with published mass deposition rates. However, since we are interested in nearest neighbors, it is imperative that our base sample be significantly complete in redshift measurements. A magnitude-limited and volume-limited subset of $R \geq 1$ Abell/ACO clusters is the only viable data set for an analysis such as this. This sample of Abell/ACO clusters has a nearly constant spatial number density ($\bar{n} = 9 \times 10^{-7}\ h_{50}^3$ Mpc^{-3}) out to $z \sim 0.10$.

After selecting an initial sample based on the above criteria, we removed any clusters which were closer to a boundary of our volume than to their nearest neighbor in order to carry out the nearest neighbor analysis described below. The remaining set of 202 clusters, which shall be referred to as AC, is a 98% complete, volume-limited sample of Abell clusters.

2.2. *The Cooling Flow Clusters*

Using the NASA Extragalactic Database, we searched the astronomical literature for papers dealing with AC clusters in order to find published determinations of $\dot{M}$. The single most comprehensive source of clusters with detailed X-ray deprojections and analysis is the 207 clusters with *Einstein* data studied by White, Jones, & Forman (1997, hereafter WJF). Our second major source is the analysis of *ROSAT* data performed by Peres et al. (1998) on a sample of the 55 X-ray brightest clusters originally identified by Edge et al. (1990). For clusters that appear in both the WJF and Peres et al. lists, we use the *ROSAT*-derived values of $\dot{M}$ from Peres et al. (taking the PSPC-derived value whenever available). A handful of additional $\dot{M}$ values were gleaned from other papers (Sarazin 1986; Edge & Stewart 1991; Pierre & Starck 1998).

All told, 55 of our AC clusters have published values of $\dot{M}$, and 26 of these have nonzero mass accretion rates (see Table 1). The fact that half our clusters with estimated $\dot{M}$ have nonzero mass accretion rates is consistent with the cooling flow occurrence rate estimated by WJF. For the analysis discussed below, we created several different subsamples of cooling flow clusters: CF1 contains only those clusters with $\dot{M} > 50\ M_\odot$ yr^{-1}, CF2 is a sample with $\dot{M} > 35\ M_\odot$ yr^{-1}, and CF3 is a sample of those clusters with $\dot{M} - \sigma_{\dot{M}} > 20\ M_\odot$ yr^{-1} (where $\sigma_{\dot{M}}$ is the estimated 1 σ lower uncertainty).

2.3. *The Non–Cooling Flow Clusters*

The WJF catalog quotes $\dot{M} = 0$ for 27 of our AC clusters. However, after taking into account the spatial resolution of the images, WJF conclude that only 10 of these are truly excluded as being cooling flows. We take these to be our most secure sample of non–cooling flow clusters (NCF1). This sample comprises A0019, A1185, A1213, A1291, A1656, A1913, A2040, A2147, A3158, and A3744. Our second sample of non–cooling flow clusters, NCF2, contains all those AC clusters in WJF which have $\dot{M} = 0$ and an upper uncertainty less than 20 $M_\odot$ yr^{-1}. After removing A2065, which has $\dot{M} \neq 0$ according to Peres et al. (1998), the NCF2 sample is made up of A0150, A0154, A0168, A0399, A0500, A0690, A1185, A1213, A1377, A1656, A1809, A1913, A2040, A2079, A2092, A2124, A2147, and A3744.

TABLE 1

THE CLUSTER COOLING FLOW SAMPLE

Cluster	$\dot{M}$ ($M_\odot$ yr^{-1})	Reference
A0085	198^{+53}_{-52}	1
A0401	42^{+82}_{-42}	1
A0970	20^{+32}_{-20}	2
A0978	500	3
A1126	500	3
A1644	11^{+40}_{-5}	1
A1650	280^{+464}_{-89}	1
A1651	138^{+48}_{-41}	1
A1795	381^{+41}_{-23}	1
A1837	12^{+29}_{-12}	2
A1983	$6^{+10.8}_{-6}$	2
A1991	37^{+36}_{-11}	2
A2029	556^{+44}_{-73}	2
A2063	37^{+7}_{-12}	1
A2065	13^{+14}_{-6}	1
A2107	$7.1^{+17.2}_{-7.1}$	2
A2151	166^{+51}_{-41}	2
A2152	20^{+13}_{-20}	2
A2197	$2.4^{+3}_{-2.4}$	2
A2199	154^{+18}_{-8}	1
A2556	81^{+105}_{-81}	2
A2657	44^{+36}_{-24}	2
A2670	41^{+71}_{-41}	2
A3112	376^{+80}_{-61}	1
A3158	25^{+74}_{-25}	1
A4059	130^{+27}_{-21}	1

NOTE.—The CF (cooling flow) sample of clusters. These are all the AC clusters with nonzero published values of $\dot{M}$. The quoted values assume $H_0 = 50$ km s^{-1} Mpc^{-1}.

REFERENCES.—(1) Peres et al. 1998; (2) WJF; (3) Sarazin 1986.

2.4. *Selection Effects*

Our AC sample is well suited for the spatial distribution analyses we are interested in. Unfortunately, the 55 AC clusters with published values of $\dot{M}$ form an inhomogeneous sample since they were observed and studied by various authors for different reasons. Nonetheless, we find (§ 3) that subsamples of cooling flow and non–cooling flow clusters drawn from this sample of clusters with known $\dot{M}$ differ significantly in their nearest neighbor distributions. It is difficult to imagine how such an effect could arise spuriously if the clusters with known $\dot{M}$ form a random sampling of the AC clusters. We point out that the clusters with known $\dot{M}$ cannot be selected from AC on the basis of an X-ray flux or luminosity cut, suggesting that they are more or less randomly selected. Although all the AC clusters are potential members of the X-ray Brightest Abell Clusters (XBACs) catalog (Ebeling et al. 1996), only 61 AC clusters and only 37 out of 55 of the AC clusters with known $\dot{M}$ meet the XBACs flux limit (even our two most massive flows do not make the catalog).

3. RESULTS

We wished to determine if the existence of cooling flows is influenced by the proximity of other clusters. We tabulated the distance to the nearest neighbor for every cluster in our AC

TABLE 2
NEAREST NEIGHBOR RESULTS

SUBSAMPLE	SUBSAMPLE SIZE	S (%)	$\overline{\text{nnd}}$ (h_{50}^{-1} Mpc)	
			Subsample	Control
CF1	12	99.8	18.4	38.4
CF2	17	95.5	28.6	38.0
CF3	14	97.6	26.0	38.0
NCF1	10	80.8	30.2	37.6
NCF2	18	89.1	29.2	38.0

NOTE.—Results of the Wilcoxon rank-sum test comparing nearest neighbor distances (nnd) of our various subsamples with the rest of the AC sample. S is the significance (%) that the subsample is systematically more crowded than the control. The average nearest neighbor distance ($\overline{\text{nnd}}$) for both the subsamples and the control samples are also tabulated.

sample and then considered whether the distribution of these nearest neighbor distances is statistically different for any of our subsamples. Since clusters are correlated, we expect these distances to be smaller than the 104 h_{50}^{-1} Mpc mean distance between our clusters. Distances to all clusters were determined assuming $q_0 = 0$ and $H_0 = 50$ km s^{-1} Mpc^{-1}.

Since we are looking for a systematic difference in the typical distance of the nearest neighbor, the Wilcoxon rank-sum test is appropriate (Lehmann & D'Abrera 1998). This test consists of putting all the nearest neighbor distances in rank order. The sum of the ranks of each subset is examined for consistency with the null hypothesis that there is no difference in the rankings. We emphasize that the significance given by this test explicitly accounts for fluctuations that may arise due to sample size.

Each subsample was compared with its own control sample made up of all the AC clusters not in that particular subsample. The results of the analysis are given in Table 2, including the significance of the result that clusters in the sample are systematically closer to their nearest neighbor than those in their control group (AC minus the subsample). Although it is not used in the assessment of significance, we also tabulate the mean distance to the nearest neighbor ($\overline{\text{nnd}}$) for each subsample and its corresponding control sample. The analysis shows one very significant result; massive cooling flows (CF1) tend to have much *nearer* closest neighbors than their control clusters. In fact, the average nearest neighbor distance ($\overline{\text{nnd}}$) is just half what it is for the remainder of the AC sample. When less massive cooling flows are included in the subsample (CF2 and CF3), the effect becomes less pronounced (although still significant at the 95% level). The significance is lowest for CF2 which, by definition, includes some clusters whose M values are consistent with zero. We performed the same analysis with the non–cooling flow samples to make sure that this is not a spurious effect. Indeed, the most secure sample of non–cooling flow clusters (NCF1) is not significantly different from the remainder of the AC sample. The second non–cooling flow sample (NCF2) contains some potential cooling flows (since $M = 0^{+20}_{-0}$) and has a higher likelihood of differing from its control sample than NCF1. This suggests a possible trend in which $\overline{\text{nnd}}$ decreases with increasing M.

As a double check, we calculated the mean number density of clusters in spheres of specified radii centered on the clusters of the entire AC sample and on those in the CF1 sample. For any given radius r, only those AC (or CF1) clusters which were at least a distance r from a boundary of the AC sample volume were considered. We used all 277 ACO clusters to find density

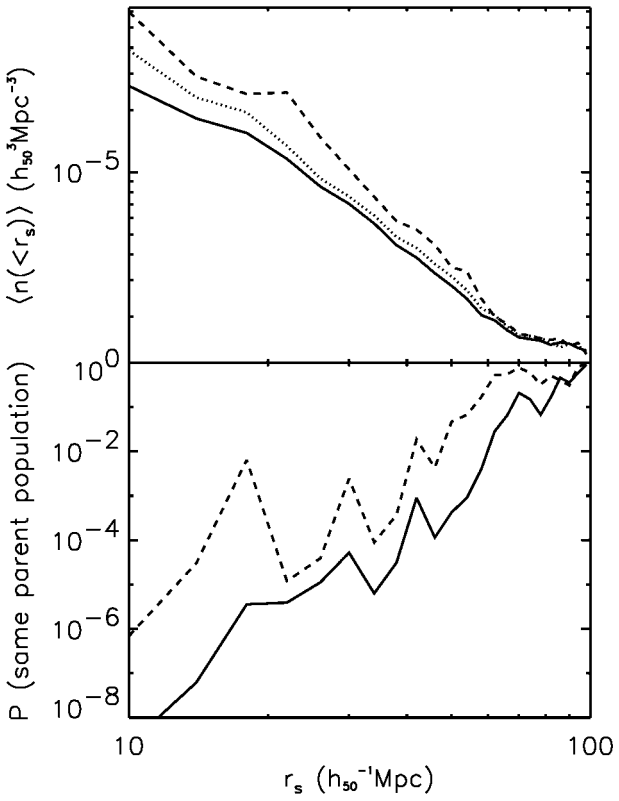

FIG. 1.—The top panel shows the mean number density of galaxy clusters in spheres of specified radii centered on the clusters in the AC sample (*solid line*), the CF1 sample (*dashed line*), and the proportioned AC sample (*dotted line*). More significantly, the bottom panel shows the probability that the densities around CF1 clusters (whose mean is shown in the upper panel) could result from a random selection of the AC sample (*solid line*) or the proportioned AC sample (*dashed line*).

inside a given radius. The results are depicted in the top panel of Figure 1 and show that local mean densities (for $r \leq 60$ h_{50}^{-1} Mpc) are higher for the CF1 clusters (*dashed line*) than for the entire AC sample (*solid line*). The significance of the difference is assessed in the bottom panel which shows the probability (using a Kolmogorov-Smirnov test; Lehmann & D'Abrera 1998) that the *distribution of densities* at a specific radius could result from a random selection of the AC parent population. The differences are highly significant out to 60 h_{50}^{-1} Mpc, although roughly what would be contributed by an average of just one extra neighbor near each CF1 cluster.

Our main result is the close nearest neighbor and generally increased density of the large-scale environment for large distances around massive cooling flow clusters. One might worry that this effect could be a richness bias as our CF1 cluster sample has a larger fraction of $R > 1$ clusters than the AC sample, causing the CF1 sample to be more strongly spatially correlated (Kaiser 1984) simply on this basis. After removing the CF1 clusters, the AC sample contains 155 $R = 1$ clusters, 33 $R = 2$ clusters, and two with $R = 3$, whereas the CF1 sample has six $R = 1$ and six $R = 2$ clusters. We therefore constructed four "proportioned" subsamples of AC that each contained all 33 of the $R = 2$ clusters as well as 33 randomly chosen $R = 1$ clusters. Averaging our Wilcoxon rank-sum test for these four samples produced a 99.5% confidence that the CF1 sample is more crowded than these richness-proportioned control groups. The mean nearest neighbor distance for the proportioned controls is 34–38 h_{50}^{-1} Mpc as opposed to

18.4 h_{50}^{-1} Mpc for CF1. This, along with the diagnostics for the proportioned set in Figure 1, indicates that the CF1 sample is significantly different from both AC and a richness-proportioned subsample of AC. We conclude that any richness bias in our result is a small effect.

4. CONCLUSIONS

We find that the most massive cooling flows (those with $\dot{M} > 50\ M_\odot\ \mathrm{yr}^{-1}$) have significantly closer nearest neighbors ($\overline{\mathrm{nnd}} = 18.4\ h_{50}^{-1}$Mpc) than the typical cluster ($\overline{\mathrm{nnd}} = 38.4\ h_{50}^{-1}$Mpc) in our complete, volume-limited sample of rich Abell clusters. We cannot exclude that this result is related to some unknown selection effect connected with why the clusters were originally selected for X-ray observation. However, this seems unlikely given that Table 2 shows a trend for the significance of the result to decrease as less massive cooling flows are added to the subsample and to disappear completely when samples of non–cooling flows are used.

How can one interpret our result that massive cooling flow clusters tend to reside in environments that are crowded with other clusters? One might expect that mergers would be much more common in such regions and that therefore cooling flows would be *less* likely to survive (see, e.g., Fabian 1994). However, it is possible that these regions are crowded because they have not yet finished collapsing and their member clusters have not recently experienced violent mergers. By this interpretation, many clusters which appear isolated may have recently gobbled up their neighbors and should show signs of dynamical activity.

Since cooling times will decrease as density increases (at fixed temperature), we might expect to find cooling flows in regions of high baryon density which would typically be regions of high matter and cluster density (Bardeen et al. 1986). However, cooling flows are found not only in clusters but also in anemic small groups and individual galaxies.

Cooling flow clusters are usually highly symmetric, indicating dynamical relaxation. Thus one might expect cooling flow clusters to be old clusters, formed from high-amplitude perturbations which collapsed early. Especially with the kind of cosmological power spectra that appear viable at this time, one would expect a high-amplitude peak to be surrounded by a larger region of high density.

We note that the density of clusters around a cooling flow cluster is significantly higher out to about 60 h_{50}^{-1} Mpc. This is interestingly close to the length scale for supercluster effects on WATs as found in Novikov et al. (1999) and to the wavelength scale going nonlinear today. It is suggestive of a general link between cooling flows and the current collapse of larger scale perturbations. It may be related to a coherent gas flow into the clusters on an even larger scale than previously suspected.

This work was supported by NSF grant AST 98-96039 (C. L.), NSF-EPSCoR (A. L. M.), and NASA-EPSCoR through the Maine Science and Technology Foundation (C. M.). We thank Keith Ashman, David Batuski, Jack Burns, Bob Nichol, and Kurt Roettiger for useful discussions.

REFERENCES

Abell, G. O. 1958, ApJS, 3, 211
Abell, G. O., Corwin, H. G., & Olowin, R. P. 1989, ApJS, 70, 1
Allen, S. W., Fabian, A. C., Edge, A. C., Bautz, M. W., Furuzawa, A., & Tawara, Y. 1996, MNRAS, 283, 263
Bahcall, N. A., Cen, R., & Gramann, M. 1994, ApJ, 430, L13
Bardeen, J. M., Bond, J. R., Kaiser, N., & Szalay, A. S. 1986, ApJ, 304, 15
Batuski, D., & Burns, J. O. 1985, ApJ, 299, 5
Bingelli, B. 1982, A&A, 107, 339
Bond, J. R., Kofman, L., & Pogosyan, D. 1996, Nature, 380, 603
Buote, D. A., & Tsai, J. C. 1996, ApJ, 458, 27
Burns, J. O., Loken, C., Gomez, P., Rizza, E., Bliton, M., & Ledlow, M. 1997, in ASP Conf. Ser. 115, Galactic and Cluster Cooling Flows, ed. N. Soker (San Francisco: ASP), 21
Burns, J. O., Roettiger, K., Ledlow, M., & Klypin, A. 1994, ApJ, 427, L87
Burns, J. O., Roettiger, K., Pinkney, J., Perley, R. A., Owen, F. N., & Voges, W. 1995, ApJ, 446, 583
Colberg, J. M., White, S. D. M., Jenkins, A., & Pearce, F. R. 1999, MNRAS, in press
Ebeling, H., Voges, W., Bohringer, H., Edge, A. C., Huchra, J. P., & Briel, U. G. 1996, MNRAS, 281, 799
Edge, A. C., & Stewart, G. C. 1991, MNRAS, 252, 428
Edge, A. C., Stewart, G. C., & Fabian, A. C. 1992, MNRAS, 258, 177
Edge, A. C., Stewart, G. C., Fabian, A. C., & Arnaud, K. A. 1990, MNRAS, 245, 559
Fabian, A. C. 1994, ARA&A, 32, 277
Fabian, A. C., & Daines, S. J. 1991, MNRAS, 252, 17P
Gomez, P. L., Loken, C., Burns, J. O., & Roettiger, K. 1999, in preparation
Kaiser, N. 1984, ApJ, 284, L9
Katgert, P., et al. 1996, A&A, 310, 8
Katz, N., & White, S. D. M. 1993, ApJ, 412, 455
Knight, P. A., & Ponman, T. J. 1997, MNRAS, 289, 955
Lehmann, E. L., & D'Abrera, H. J. M. 1998, Nonparametrics (San Francisco: Holden-Day)
McGlynn, T. A., & Fabian, A. C. 1984, MNRAS, 208, 709
Miller, C. J., Batuski, D. J., Slinglend, K.,& Hill, J. 1999a, ApJ, in press
Miller, C. J., Krughoff, K. S., Batuski, D. J., Slinglend, K. A., & Hill, J. H. 1999b, in preparation
Novikov, D. I., Melott, A. L., Wilhite, B. C., Kaufman, M., Burns, J. O., Miller, C. J., & Batuski, D. J. 1999, MNRAS, 304, L5
Pauls, J., & Melott, A. L. 1995, MNRAS, 274, 99
Peacock, J. A., & West, M. J. 1992, MNRAS, 259, 494
Peres, C. B., Fabian, A. C., Edge, A. C., Allen, S. W., Johnstone, R. M., & White, D. A. 1998, MNRAS, 298, 416
Pierre, M., & Starck, J.-L. 1998, A&A, 330, 801
Plionis, M. 1994, ApJS, 95, 401
Sarazin, C. L. 1986, Rev. Mod. Phys., 58, 1
Sarazin, C. L., Burns, J. O., Roettiger, K., & Mcnamara, B. R. 1995, ApJ, 447, 559
Shandarin, S. F., & Klypin, A. A. 1984, Soviet Astron., 28, 491
Slinglend, K. A., Batuski, D. J., Miller, C. J., Haase, S., Michaud, K., & Hill, J. M. 1998, ApJS, 115,1
West, M. J., Jones, C., & Forman, W. 1995, ApJ, 451, L5
White, D. A., Jones, C., & Forman, W. 1997, MNRAS, 292, 419 (WJF)